Excess Noise Factor of a-Si:H/a-SiC:H Separated Absorption and Multiplication Region Superlattice-like Avalanche Photodiodes (SAM-SAPDs)

Neng-Fu Shih[1] , Huei -Ching Huang[2], Chung-Yuan Kung[2], Chun-Chih Chiu[3], and Jyh-Wong Hong[3]

[1] Dept. of Electronics Engineering, Hsiuping Institute of Technology No.11, Gungye Rd., Dali, Taichung, 412, Taiwan, R. O. C.
[2] Dept. of Electrical Engineering, National Chung Hsing University, Taichung, Taiwan, R. O. C.
[3] Dept. of Electrical Engineering, National Central University, Chungli32054, Taiwan, R. O. C.

Abstract

In this paper, an a-Si:H/a-SiC:H separated absorption and multiplication region superlattice avalanche photodiode (SAM-SAPD) using combined effect of band edge discontinuity and build-in potential in p-n junction is designed and fabricated successfully. The formula that describe the relationships among excess noise factor (F_e), mean multiplication ($\langle M_e \rangle$), and the ionization rate ratio (k_s) for this SAM-SAPD are established theoretically. The comparisons between the theoretical calculations and the experimental results for F_e vs. M_e are discussed.

Keywords: excess noise factor, mean multiplication, ionization rate.

1. Introduction

For long-range optical communications while weak light is able to be detected, it is desirable to use a detector with high sensitivity, low dark current, fast response speed, and very high optical gain [1]. In general, large optical gain could be obtained in an avalanche photodiode (APD). The excess noise of APD is an important parameter needs to be considered for making a good device. Low excess noise can be obtained when the electron and hole impact ionization rates differ greatly [2].

Artificially enhancing the ratio of electron to hole impact ionization rates can be conducted by the following way: potential step discontinuities as in a multiple quantum well/ superlattice structure[3]; built-in electric field arising from fully depleted p-i-n[4,5], p-n homo-junction[6], or p-n hetero-junction in conjunction with a band edge discontinuity[7]; impact ionization of electrons from confined quantum well states; or even by use of separated absorption and multiplication layers (SAM).

In this study, we have designed and fabricated an i-a-Si:H/i-a-SiC:H SAM-SAPD to investigate the relation between excess noise factor (F_e) versus mean multiplication $<M_e>$ experimentally. We also established a theoretical calculation on SAM-SAPD for $<M_e>$ and F_e. Comparing the results between the theoretical calculations and measured experimental data, the device character of SAM-SAPD seems to be more clearly.

2. Fabrication process and experimental results

The employed substrate was ITO-coated Corning 7059 glass. After the standard cleaning process, the substrate was put into the ULVAC CPD-1108D plasma-enhanced chemical vapor deposition (PECVD) system and the chamber was completely pumped down to 4×10^{-6} torr or lower. After the heating cleaning process (250℃, 90minutes), the various amorphous films were deposited on the substrate.

The schematic cross section and the gas flow-rate for the amorphous SAM-SAPD with additional p-a-SiC:H/i-a-SiC:H/n-a-SiC:H/i-a-Si:H/i-a-SiC:H layers are shown in Fig. 1. To avoid carbon contamination in a-Si:H layers, the glow-discharge was turned off at the end of each a-SiC:H layer deposition, and then the chamber was completely pumped down for 5 minutes before depositing the next layer.

After depositing the various amorphous layers, the samples were put into an E-beam coater, then the 200nm Al top electrodes were deposited onto the n^+-a-Si:H layer. The diameter of the electrode defined by the circular metal mask was 1.2 mm. After that, the sample was Rapid Thermal Annealed at 300℃ for 10 minutes. The RTA chamber was filled with pure H_2 and kept at 1atm. The raising rate of temperature was set to be 10℃/s, and cooled down to room temperature naturally.

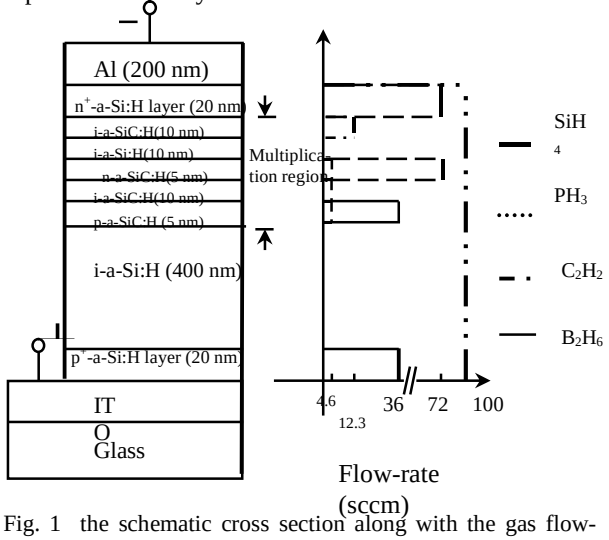

Fig. 1 the schematic cross section along with the gas flow-rates for the amorphous SAM-SAPD with additional p-i-n-i-i

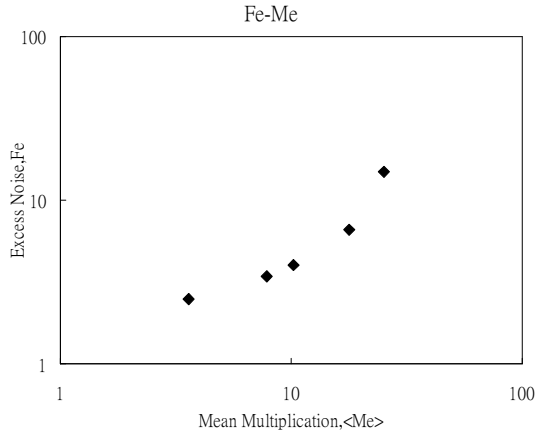

Fig. 2 the excess noise factor vs. multiplication for the proposed SAM-SAPD (k_s=0.252).

The relationships of excess noise factor versus mean multiplication for the SAM-SAPD are shown in Fig. 2. The noise spectral density was measured using an HP-3562A dynamic signal analyzer through a bias tee via a current amplifier. The ionization rate ratio of this device is 0.252.

3. Theoretical calculations

Here we quote the theory presented by Shih [8] to simulate the relationships between excess noise factor (F_e) and mean multiplication (<M_e>). The energy-band diagram of a SAM-SAPD is shown in Fig.3 [8]. The α_i and β_i are the symbols for electron and hole ionization coefficients in the *i*th substage, respectively, and *g* is the dark carrier generation rate. The width of the depletion region *mL* is consisted of spatial replications of an arbitrary number *m* of identical stages. Each stage has total width *L* and consists of an arbitrary number N of substages. Each substage is characterized by its width L_i. The absorption region and avalanche region widths are w and d respectively.

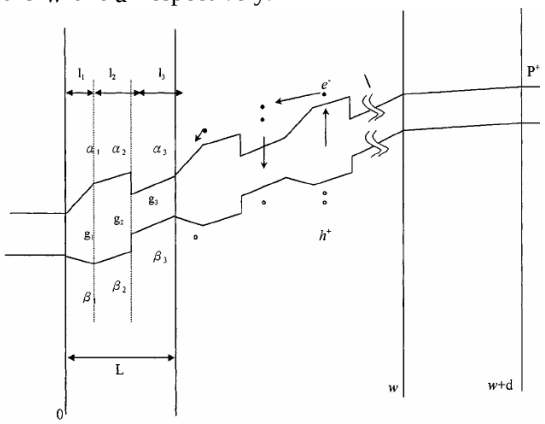

Fig.3 The energy-band diagram of SAM-SAPD. [8]

A. SAPD

In Fig. 3, when *d* is set to zero, the energy-band diagram becomes to be a superlattice-like structure APD (SAPD). Let $M(x)$ be the average number of electron-hole pairs resulting from an initial pair generated at position x in the depletion region (see Fig.3). For photo-carriers injected at w, $M(w)$ can be expressed as following [9]

$$M(w) = \frac{1}{1 - \frac{R(1-R^m)}{1-R}\sum_{i=1}^{N}\frac{\alpha_i}{\beta_i - \alpha_i}Hi} \tag{1}$$

Where $H_i = \exp\left(\sum_{j=1}^{i-1}(\alpha_j - \beta_j)l_j\right)\left[1-\exp((\alpha_i-\beta_i)l_i)\right]$,

$$\frac{M(nL)}{M((n+1)L)} = \frac{1+Q}{1+P} = \frac{1+ksP}{1+P} \equiv R$$

$$P = \exp\left(\sum_{i=1}^{N}\alpha_i l_i\right) - 1\ ,\ Q = \exp\left(\sum_{i=1}^{N}\beta_i l_i\right) - 1\ ,$$

We define the ionization rate ratio k_s=Q/P. The mean dark multiplication < M_d> is [10]

$$< M_d >= M(w)\frac{\frac{R(1-R^m)}{1-R}\sum_{i=1}^{N}\frac{g_i}{\beta_i-\alpha_i}Hi}{m\sum_{i=1}^{N}g_i l_i} \tag{2}$$

In the general case, both dark-generated and injected carriers exist, these give rise to the currents I_d and I_e, respectively. Therefore, a mixed injection current is $I_m = I_e + I_d$, which leads to a total multiplied current

$$I = I_m\langle M_e\rangle = I_e M(w) + I_d\langle M_d\rangle,$$

where $\langle M_e\rangle$ is the mixed multiplication.

The current consists of two components: the electron current I_n and the hole current I_p. The increase in the hole current in an infinitesimal length *dx* at point *x* in the sum of the multiplied electron current and the multiplied hole current plus the current associated with dark generation [11], we obtain

$$dI_p = (\alpha I_n + \beta I_p + g)dx \tag{3}$$

In general, for substage *i* in the *n*th stage, the general expression for the current is

$$\begin{aligned} I_n(x) = &\left\{ I_n(nL)\exp\left[\sum_{j=1}^{i-1}(\beta_j - \alpha_j)l_j\right]\right. \\ &- \sum_{j=1}^{i-1}\frac{\beta_j I + g_j}{\beta_j - \alpha_j}\left[\exp((\beta_j - \alpha_j)l_j) - 1\right] \\ &\left.\cdot\exp\left[\sum_{k=j+1}^{i-1}(\beta_k - \alpha_k)l_k\right] - \frac{\beta_i I + g_i}{\beta_i - \alpha_i}\right\} \\ &\cdot\left[\exp(\beta_j - \alpha_j)(x - nL - L_{i-1})\right] + \frac{\beta_i I + g_i}{\beta_i - \alpha_i} \end{aligned} \tag{4}$$

For electron injection only, $I_n(w) = I_n(mL) = I_e$. This lead to

$$I_n(nL) = \frac{R(1-R^{n-m})}{R-1}\sum_{i=1}^{N}\frac{\beta_i I + g_i}{\beta_i - \alpha_i}H_i + R^{n-m}I_e \tag{5}$$

The multiplication noise in APDs is characterized by the excess noise factor. Using the relationship between the excess noise factor and the current spectral density obtained by Teich et al.[9], and assuming the statistical properties of the carrier-pair generation is Poisson process, we find spectral noise

density

$$S_m = 2e\langle I_m\rangle\langle M_e\rangle^2 F_e \tag{6}$$

where F_e is the excess noise factor. The spectral noise component arising in $[x, x+dx]$ is [9]

$$dS_m = 2eM^2(x)\,\mathrm{var}(dI_p(x)) = 2eM^2(x)dI_p(x) \tag{7}$$

Integrating this expression, we obtain [9]

$$\begin{aligned}\frac{S_m}{2e} &= M^2(w)I_e\left[1-\frac{R(1-R^m)}{1-R}\sum_{n=1}^{N}H_n\right]\\ &+M^2(w)\frac{R(1-R^m)}{1-R}\sum_{n=1}^{N}\frac{\beta_n I+g_n}{\beta_n-\alpha_n}H_n\\ &\times\left\{\frac{R}{R-1}\sum_{i=1}^{N}H_i-\frac{R(1+R^m)}{1+R}\left[\frac{R}{R-1}\sum_{i=1}^{N}H_i\right.\right.\\ &\left.\left.-\exp(\sum_{i=1}^{n-1}(\alpha_i-\beta_i)l_i)-\sum_{i=n+1}^{N}H_i\right]\right\}\end{aligned} \tag{8}$$

B. SAM-SAPD

The energy-band diagram of a SAM-SAPD is shown in Fig. 3[8].Use α 'and β ' as the symbols for electron and hole ionization rate in the absorption region , respectively , $g'$is the dark carrier generation rate and the width of reach-through region is *d*. The photocarriers injected at $w+d$, the mean multiplication can be expressed as

$$M(w+d)=1+\frac{\frac{R(1-R^m)}{1-R}\sum_{i=1}^{N}\frac{\alpha_i}{\beta_i-\alpha_i}H_i+\frac{\alpha'}{\beta'-\alpha'}\left[1-e^{(\alpha'-\beta')d}\right]}{1-\frac{R(1-R^m)}{1-R}\sum_{i=1}^{N}\frac{\alpha_i}{\beta_i-\alpha_i}H_i} \tag{9}$$

The mean dark multiplication $\langle M_d\rangle$ is [8]

$$\langle M_d\rangle=\frac{M(w)\left\{\frac{R(1-R^m)}{1-R}\sum_{i=1}^{N}\frac{g_i}{\beta_i-\alpha_i}H_i+\frac{g'}{\beta'-\alpha'}\left[1-e^{(\alpha'-\beta')d}\right]\right\}}{m\sum_{i=1}^{N}g_i l_i+g'd} \tag{10}$$

where $M(w)=M(w+d)\exp(\beta'-\alpha')d$. Similarly, the spectral noise density of absorption structure can be expressed as

$$\begin{aligned}\frac{S_m}{2e} &= \int_0^w M^2(x)[(\alpha-\beta)I_n(x)+(\beta I+g)]dx\\ &+\int_w^{w+d}M'^2(x)[(\alpha'-\beta')I'_n(x)+(\beta' I+g')]dx\\ &= S_1+S_2\end{aligned} \tag{11}$$

S_1 is similar to (8) except that I_e is substituted by $I_n(w)$ and $M(w)=M(w+d)\exp(\beta'-\alpha')d$. The current equation is [8]

$$I_n(w)=\left[I_e-\frac{\beta' I+g'}{\beta'-\alpha'}\right]e^{(\alpha'-\beta')d}+\frac{\beta' I+g'}{\beta'-\alpha'} \tag{12}$$

S_2 can be expressed as

$$\frac{S_2}{2e}=\frac{1}{2}M^2(w)\left[I_e-\frac{\beta' I+g'}{\beta'-\alpha'}\right]\left[e^{2(\alpha'-\beta')d}-1\right] \tag{13}$$

Combine these equations, we obtain

$$\begin{aligned}\frac{S_m}{2e} &= M^2(w)\left\{\left[Ie-\frac{\beta' I+g'}{\beta'-\alpha'}\right]\exp(\beta'-\alpha')d+\frac{\beta' I+g'}{\beta'-\alpha'}\right\}\cdot\\ &\left[1-\frac{R(1-R^m)}{1-R}\sum_{n=1}^{N}H_n\right]+M^2(w)\frac{R(1-R^m)}{1-R}\sum_{n=1}^{N}\frac{\beta_n I+g_n}{\beta_n-\alpha_n}H_n\\ &\times\left\{\frac{R}{R-1}\sum_{i=1}^{N}H_i-\frac{R(1+R^m)}{1+R}\left[\frac{R}{R-1}\sum_{i=1}^{N}H_i\right.\right.\\ &\left.\left.-\exp(\sum_{i=1}^{n-1}(\alpha_i-\beta_i)l_i)-\sum_{i=n+1}^{N}H_i\right]\right\}\\ &+\frac{1}{2}M^2(w)\left[Ie-\frac{\beta' I+g'}{\beta'-\alpha'}\right]\left[(\exp 2(\beta'-\alpha')d)-1\right]\end{aligned} \tag{14}$$

where $M(w)=M(w+d)\exp(\beta'-\alpha')d$.

Equations (9) and (14) in SAM-SAPD can be simplified to equations (1) and (8) in SAPD when d set to zero.

4. Result and discussion

The experimental data and theoretical deductions are exhibited in section 2 and section 3, respectively. In order to prove that the theoretical calculations can fit well with the experimental data, we make the estimation on the ionization coefficients for each layer of the SAM-SAPD and also for the absorption region.

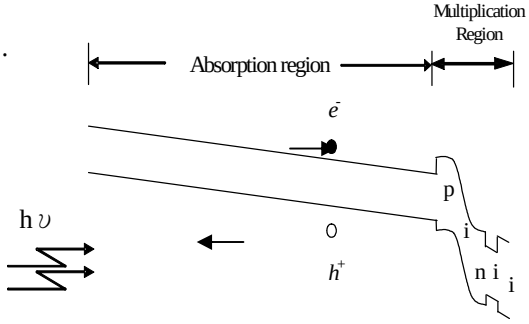

Fig. 4 the energy-band diagram for the SAM-SAPD

The energy-band diagram under reverse bias for the SAM-SAPD is shown in Fig. 4. When a photon is absorbed in the absorption region, it generates an electron-hole pair. After that the electron enters the multiplication region. If the electron drifts to the narrower band-gap material layer from the wider band-gap material layer, it gets an excess kinetic energy by conduction band offset ($\triangle E_c$), i.e. the electron obtains the excess kinetic energy only when it enters to a-Si:H layer from a-SiC:H layer, then it would lose the energy by impact ionize process. Therefore, we assume that electron ionization coefficient of the narrower band-gap layer is larger than the wider band-gap layer. However, if the electron exists in some layer whose band-gap is narrower than the next layer, it experiences an energy barrier, so the electron ionization coefficient of the next layer is inferred as zero or a tiny value. The corresponding lengths, the assumed electron and the assumed hole ionization coefficients of the proposed device are listed in Table 1.

Table1. Lengths and ionization coefficients of each layer

	Substage (i)	1	2	3	4	5
ks=0.05	Length (l_i)	5nm	5nm	5nm	10nm	10nm
	Electron ionization coefficient (α_i)	0 cm^{-1}	2550 cm^{-1}	1700 cm^{-1}	2125 cm^{-1}	0 cm^{-1}
	Hole ionization coefficient (β_i)	16 cm^{-1}	144 cm^{-1}	0 cm^{-1}	80 cm^{-1}	64 cm^{-1}
ks=0.2	Length (l_i)	5nm	5nm	5nm	10nm	10nm
	Electron ionization coefficient (α_i)	0 cm^{-1}	630 cm^{-1}	420 cm^{-1}	1000 cm^{-1}	0 cm^{-1}
	Hole ionization coefficient (β_i)	16 cm^{-1}	144 cm^{-1}	0 cm^{-1}	80 cm^{-1}	64 cm^{-1}

The avalanche process in the absorption region is significant. Using the parameters in Table 1 and the mathematical expressions, equation (8) and (14) in section 3, the calculated results for excess noise factor versus mean multiplication can be obtained. There might have two situations in the absorption region. First situation, the absorption region in SAM-SAPD is free of avalanche process. In this case, avalanche only occurs in the multiplication region, equation (8) is suitable for simulating the excess noise factor versus the mean multiplication. Second situation, the avalanche process takes place both in the multiplication and absorption region, but the electron and hole ionization coefficients in the absorption region is very small. Equation (14) is used for calculating the excess noise factor versus the mean multiplication. Fig. 5 represents the simulation results using both equation (8) and (14) with various k_s values. Since equation (8) is much better than equation (14) in the fitting of experimental result indicates that there is no avalanche process in the absorption region of SAM-SAPD.

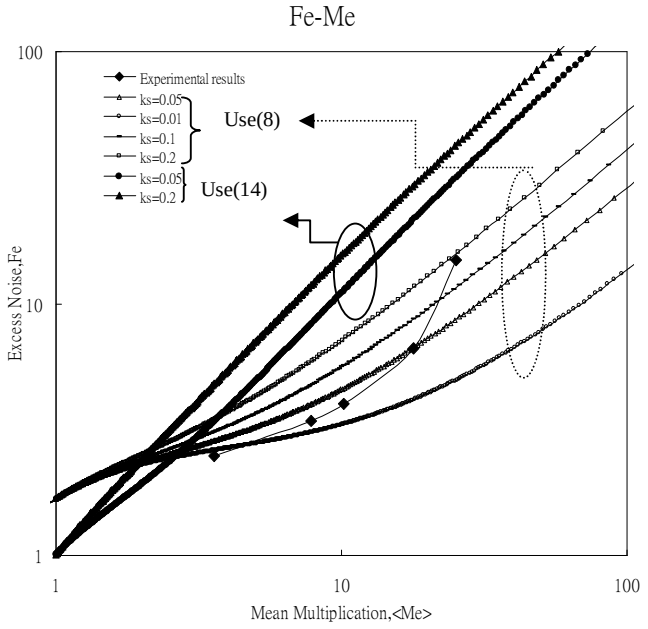

Fig. 5 comparisons of experimental results (k_s=0.252) and calculated results. Filled diamonds indicate the experimental results.

5. Summary

We have designed a SAM-SAPD with simple structure and lower process cost. The relations of F_e vs. $\langle M_e \rangle$ were also discussed by theoretical simulations and experimental measurements in this paper. The simulation results approach to the experimental results reasonably in terms of F_e vs. $\langle M_e \rangle$; hence, the validities of the theoretical expressions [8] can be proved. Through the various assumptions, we suspect that the avalanche processes only occur in the multiplication region of this SAM-SAPD.

6. References

[1] K. H. Lee, Y. K. Fang, and G. Y. Lee, " A Normal Amorphous Silicon-Based Separate Absorption and Multiplication Avalanche Photodiode (SAMAPD) with Very High Optical Gain," *IEEE Trans. Electron Devices*, vol.40,pp.1929-1933,1995.

[2] R. J. McIntyre, "Multiplication noise in uniform avalanche diodes,"*IEEE Trans. Electron Devices*, vol. ED-13, pp. 164–168, 1966.

[3] H. Blauvelt, S. Margalit, and A. Yariv, "Single-carrier-type dominated impact ionization in multilayer structures," *Electron. Lett.*, vol. 18, pp.375-376,1982.

[4] K. Brennan, "Theory of the GaInAs/A1InAs-doped quantum well APD: A new low-noise solid-state photodetector for lightwave communication systems, "*IEEE Trans. Electron Devices*, vol. ED-33, 1653-1695,1986.

[5] K. Brennan, "Theory of the doped quantum well superlattice APD: A new solid state photomultiplier," *IEEE J. Quantum Electron*., vol. QE-22, pp. 1999-2016, 1986.

[6] K. Brennan, "The pn junction quantum well APD: A new solid state Photodetector for lightwave communications systems and on-chip detector applications," *IEEE Trans. Electron Devices*, vol. ED-34, pp. 782-792, 1987.

[7] K. Brennan, "The p-n heterojunction quantum well APD: A new high-gain low-noise high-speed photodetector suitable for lightwave communications and digital applications,"*IEEE Trans. Electron Devices*, vol. ED-34, pp. 793-803,1987.

[8] N. F. Shih, "Excess Noise Analysis of Separate Absorption Multiplication Region Superlattice Avalanche Photodiodes," I*EEE Trans. Electron Devices*, Vol. 48, no. 6, pp.1075-1081, 2001

[9] M. C. Teich, K. Matsuo, and B. E. A. Saleh, "Excess noise factors for conventional and superlattice avalanche photodiodes and photomultiplier tubes," *IEEE J. Quantum Electron.*, vol. QE-22, pp. 1184–1193, 1986.

[10] N. Z. Hakim, B. E. A. Saleh, and M. C. Teich, "Generalized excess noise factor for avalanche photodiodes of arbitrary structure," *IEEE Trans.Electron Devices*, vol. 37, pp. 599–610, 1990.

[11] K. F. Brennan, Y. Wang, M. C. Teich, B. E. A. Saleh, and T. Khorsandi, "Theory of the temporal response of a simple multiquantum-well avalanche photodiode," *IEEE Trans. Electron Devices*, vol. 35, pp.1456–1467, 1988.